

Latent Space-based Likelihood Estimation Using Single Observation for Bayesian Updating of Nonlinear Hysteretic Model

Sangwon Lee^a, Taro Yaoyama^b, Yuma Matsumoto^d, Takenori Hida^e, Tatsuya Itoi^f

^aProject researcher Department of Architecture Graduate School of Engineering The University of Tokyo Tokyo Japan

^bProject Assistant Professor Department of Architecture Graduate School of Engineering The University of Tokyo Tokyo Japan

^cPh.D student Department of Architecture Graduate School of Engineering The University of Tokyo Tokyo Japan

^dResearch Fellow of Japan Society for the Promotion of Science Tokyo Japan

^eAssociate Professor Major in Urban and Civil Engineering Graduate School of Science and Engineering Ibaraki University Ibaraki Japan

^fAssociate Professor Department of Architecture Graduate School of Engineering The University of Tokyo Tokyo Japan

Abstract

This study presents a novel approach to quantifying uncertainties in Bayesian model updating, which is effective in sparse or single observations. Conventional uncertainty quantification metrics such as the Euclidean and Bhattacharyya distance-based metrics are potential in scenarios with ample observations. However, their validation is limited in situations with insufficient data, particularly for nonlinear responses like post-yield behavior. Our method addresses this challenge by using the latent space of a Variational Auto-encoder (VAE), a generative model that enables nonparametric likelihood evaluation. This approach is valuable in updating model parameters based on nonlinear seismic responses of structure, wherein data scarcity is a common challenge. Our numerical experiments confirm the ability of the proposed method to accurately update parameters and quantify uncertainties using limited observations. Additionally, these numerical experiments reveal a tendency for increased information about nonlinear behavior to result in decreased uncertainty in terms of estimations. This study provides a robust tool for quantifying uncertainty in scenarios characterized by considerable uncertainty, thereby expanding the applicability of Bayesian updating methods in data-constrained environments.

1. Introduction

Analytical models that describe the behavior of an existing structure require periodic updates throughout its lifetime to accurately predict its realistic performance. This need arises from the changing state of the structure caused by factors such as deterioration or damage due to seismic events. Common practice entails observational data for these updates that reflects the current condition of the structure.

Numerous conventional methods for such model updating refine the model deterministically to best fit the data. In this field, sensitivity-based approaches (Collins et al., 1974; Mottershead et al., 2011) have received great attention while there has been development in frequency response methods (Imregun et al., 1995; Sipple and Sanayei, 2014). These techniques are useful for assessing events including evaluating damage caused by earthquakes, especially in well-posed situations wherein the problem is well-defined and the solutions are stable. Although this deterministic approach is effective to evaluate such existing damage, it may introduce biases when used for future predictions. Intricate systems, such as structural systems, are riddled with uncertainties that possess nondeterministic features (Goldstein, 2006). Precise model-based predictions necessitate the resolution of these uncertainties (Volodina and Challenor, 2021). Hence, there

is a growing interest in probabilistic methods that adequately account for these uncertainties during model updating. Amidst these probabilistic methodologies, the Bayesian method is receiving increasing recognition for its effectiveness in dealing with these uncertainties.

The Bayesian approach operates on the principle of updating beliefs based on new evidence. Initial or prior probability is established, based upon existing knowledge or beliefs. As new data become available, the prior probability is combined with the likelihood of newly observed data. This process produces an updated posterior probability which later becomes the new prior for subsequent observations, thereby facilitating a continuous update of beliefs as more data is obtained. This distinct mechanism seamlessly integrates prior knowledge with newly obtained data within the Bayesian methodology.

Within this framework, the likelihood evaluation, which quantifies uncertainty and evaluates the probability of observed data based on a specific hypothesis, is the crucial transition from prior to posterior probabilities. This evaluation ensures the accurate updating of posterior probabilities, thereby resulting in more robust and reliable predictions.

Numerous studies have been conducted on model updating using the Bayesian approach. Among these studies, notable approaches (Beck and Katafygiotis, 1998; Yang et al., 2023; Saito, 2013; Saito and Beck, 2010) assume a specific distribution form for the likelihood function. Although utilizing simple distributions like the normal distribution makes it computationally convenient, it is not immune to potentially unrealistic assumptions. Alternatively, distance-based metrics (Bi et al., 2017), including approaches that leverage the Bhattacharyya distance (Bhattacharyya, 1946), are employed in nonparametric methods, showing promise when a substantial amount of data is available (Bi et al., 2019; Kitahara et al., 2022, 2021). Obtaining a considerable amount of data, particularly for nonlinear structural responses, is a formidable task. Hence, updating nonlinear hysteretic models has primarily relied on deterministic methods (Song et al., 2018) or methods that assume a specific distribution form for the likelihood function (Hinze et al., 2020).

This study presents a novel approach for nonparametric likelihood estimation aimed to quantify uncertainties in Bayesian model updating. The emergence of nonparametric methods that facilitate the nonparametric likelihood estimation of nonlinear hysteretic models with minimal data can revolutionize model updating. This advancement would enhance the robustness and generalization capabilities of the Bayesian model updating for uncertain future predictions.

2. Methodology

2.1. Overview of Bayesian Updating for Nonlinear Systems

2.1.1. Nonlinear system & feature sample

In model updating involving uncertainty quantification, a linear system is often used to model the actual structure. This includes three elements: the model parameter θ , output feature \mathbf{x} , and the simulator function $h_l(\cdot)$, which are expressed as:

$$\mathbf{x} = h_l(\theta) \quad (1)$$

where $\mathbf{x} = [x_1, x_2, \dots, x_m]^T$; $\theta = [\theta_1, \theta_2, \dots, \theta_n]^T$; m and n represent the element size of the output feature \mathbf{x} and the model parameter θ , respectively. The output feature includes the structural parameters such as natural vibration frequencies or vibration modes, while a linear simulator $h_l(\cdot)$ includes method such as seismic linear response analysis.

In the case of model updating of a nonlinear system that models the nonlinear seismic response of an existing structure, the nonlinear system can be characterized as:

$$\mathbf{x} = h(\theta | u) \quad (2)$$

Here, the nonlinear simulator $h(\cdot)$ is interpreted as the output from the nonlinear seismic response analysis, with u representing the input ground motion. Example of output feature from the nonlinear seismic response analysis is a discretized frequency response function of response, which depends on the model parameter θ .

To update the model parameters, the observed features are required. Suppose the number of observation is N_{obs} , the observed feature sample $\mathbf{X}_{\text{obs}} \in \mathbb{R}^{m \times N_{\text{obs}}}$ is expressed as:

$$\mathbf{X}_{\text{obs}} = [\mathbf{x}_1, \mathbf{x}_2, \dots, \mathbf{x}_{N_{\text{obs}}}] \quad (3)$$

2.1.2. Bayes updating

The Bayesian updating is performed by evaluating the conditional probabilities of the parameters based on the observed feature sample $p(\theta|\mathbf{X}_{\text{obs}})$ expressed as:

$$p(\theta|\mathbf{X}_{\text{obs}}) = \frac{p(\mathbf{X}_{\text{obs}}|\theta) p(\theta)}{p(\mathbf{X}_{\text{obs}})} \quad (4)$$

where

- $p(\theta|\mathbf{X}_{\text{obs}})$ is the posterior distribution representing the updated knowledge based on the observational data;
- $p(\mathbf{X}_{\text{obs}}|\theta)$ is the likelihood function of \mathbf{X}_{obs} for an instance of θ ;
- $p(\theta)$ is a prior distribution representing initial knowledge about θ ;
- $p(\mathbf{X}_{\text{obs}})$ is the normalization factor that ensures that the posterior distribution integrates to unity.

Considering that $p(\mathbf{X}_{\text{obs}})$ is a constant, the posterior distribution can be expressed as follows:

$$p(\theta|\mathbf{X}_{\text{obs}}) \propto p(\mathbf{X}_{\text{obs}}|\theta) p(\theta) \quad (5)$$

Using Markov Chain Monte Carlo (MCMC) methods, samples from the posterior $p(\theta|\mathbf{X}_{\text{obs}})$ can be obtained. Assuming that the prior distribution $p(\theta)$ is obtained from prior information, only the likelihood $p(\mathbf{X}_{\text{obs}}|\theta)$ must be known from the observation.

Based on sufficient observational data, updating can be directed towards minimizing the stochastic distance between the observed and simulated samples. Here, the likelihood function can be set as follows (Bi et al., 2019; Kitahara et al., 2022):

$$p(\mathbf{X}_{\text{obs}}|\theta) = \exp \left\{ -\frac{d(\mathbf{X}_{\text{obs}}, \mathbf{X}_{\text{sim}})^2}{\epsilon} \right\} \quad (6)$$

where \mathbf{X}_{sim} represents the simulated feature sample and $d(\cdot, \cdot)$ is a stochastic distance, such as the Bhattacharyya distance. ϵ represents the width factor, and is a hyperparameter influencing the breadth of the posterior distribution. Suppose the required size of the samples is N_{sim} , the simulator $h(\cdot)$ is executed N_{sim} times to generate the simulated feature sample $\mathbf{X}_{\text{sim}} \in \mathbb{R}^{m \times N_{\text{sim}}}$, which can be expressed as:

$$\mathbf{X}_{\text{sim}} = [\mathbf{x}_1, \mathbf{x}_2, \dots, \mathbf{x}_{N_{\text{sim}}}] \quad (7)$$

The number of simulations N_{sim} is determined to ensure an accuracy of $p(\mathbf{X}_{\text{obs}}|\theta)$. However, obtaining the satisfactory number of observation N_{obs} remains challenging. It is often the case that there is limited observed data available. For example, when updating parameters related to the nonlinear structural response during seismic excitation, the number of observations N_{obs} is generally few over the lifetime of the structure. Such sparse but valuable data can be perceived as outliers in the conventional model updating method, because it may have a negligible impact on the accuracy of model updating. Hence, it is crucial to develop a method that quantifies uncertainties from limited data aimed at updating parameters related to such nonlinear seismic response.

2.2. Novel Likelihood Evaluation Method

The likelihood $p(\mathbf{X}_{\text{obs}}|\theta)$, as represented in Eq. (5), is expressed as:

$$p(\mathbf{X}_{\text{obs}}|\theta) = p(\mathbf{X}_{\text{obs}}|\mathbf{X}_{\text{sim}}) \quad (8)$$

Using an arbitrary multidimensional random variable \mathbf{z} , $p(\mathbf{X}_{\text{obs}}|\mathbf{X}_{\text{sim}})$ can be expressed as the marginalization of $p(\mathbf{X}_{\text{obs}}|\mathbf{z})$ as follows:

$$p(\mathbf{X}_{\text{obs}}|\mathbf{X}_{\text{sim}}) = \int_{\mathcal{Z}} p(\mathbf{X}_{\text{obs}}|\mathbf{z}) p(\mathbf{z}|\mathbf{X}_{\text{sim}}) d\mathbf{z} \quad (9)$$

where $\mathbf{z} = [z_1, z_2, \dots, z_{z_{\text{dim}}}]^T \in \mathcal{Z}$. It is assumed that \mathbf{X}_{obs} and \mathbf{X}_{sim} are conditionally independent given \mathbf{z} . Because \mathbf{z} is a non-unique random variable, it is advantageous to set a manageable random variable \mathbf{z} among the possible as discussed later.

By transforming $p(\mathbf{X}_{\text{obs}}|\mathbf{z})$ using Bayes' theorem and Eq. (8), the likelihood $p(\mathbf{X}_{\text{obs}}|\theta)$ is expressed as follows:

$$p(\mathbf{X}_{\text{obs}}|\theta) = c \int_{\mathcal{Z}} \frac{p(\mathbf{z}|\mathbf{X}_{\text{obs}}) p(\mathbf{z}|\mathbf{X}_{\text{sim}})}{p(\mathbf{z})} d\mathbf{z} \quad (10)$$

In Eq. (10), $p(\mathbf{X}_{\text{obs}})$ is a constant and is denoted as c . If the probability distribution of \mathbf{z} and the two conditional probabilities of \mathbf{z} are obtained, the likelihood $p(\mathbf{X}_{\text{obs}}|\theta)$ is obtained using Eq. (10).

In this context, the actual probability density function, $p(\mathbf{z}|\cdot)$, is intractable (Kingma and Welling, 2014). A numerical approach can be used to obtain the value of the likelihood $p(\mathbf{X}_{\text{obs}}|\theta)$ by approximating $p(\cdot)$ by $q(\cdot)$ as expressed as follows:

$$p(\mathbf{X}_{\text{obs}}|\theta) \approx c \int_{\mathcal{Z}} \frac{q(\mathbf{z}|\mathbf{X}_{\text{obs}}) q(\mathbf{z}|\mathbf{X}_{\text{sim}})}{q(\mathbf{z})} d\mathbf{z} \quad (11)$$

It is difficult to find the proportionality constant c here, but for MCMC it is sufficient to know the proportional value of the likelihood.

\mathbf{z} is a non-unique random variable. If \mathbf{z} follows a low-dimensional and manageable distribution, \mathbf{z} and \mathcal{Z} represent the latent variable and latent space, respectively. This latent space captures hidden features or structures in data and plays a crucial role in complex data analysis. Here, \mathbf{z} is a key parameter for quantifying the similarity between the observed feature sample \mathbf{X}_{obs} and the simulated feature sample \mathbf{X}_{sim} . The utilization of the latent space enables in depth analysis of data, and Eq. (11) expresses the complex relationships between data using these latent features.

2.3. Application of VAE for Likelihood Estimation

As regards a practical example, this section shows an approach that utilizes the encoder of VAE (Kingma and Welling, 2014) as a probabilistic model that generates the output $q(\cdot)$. An overview of VAE is provided in Appendix Appendix A. Using $q_{\phi}(\cdot)$ as a substitute for $q(\cdot)$ in Eq. (11) enables the evaluation of the likelihood as expressed as follows:

$$p(\mathbf{X}_{\text{obs}}|\theta) \approx c \int_{\mathcal{Z}} \frac{q_{\phi}(\mathbf{z}|\mathbf{X}_{\text{obs}}) q_{\phi}(\mathbf{z}|\mathbf{X}_{\text{sim}})}{q_{\phi}(\mathbf{z})} d\mathbf{z} \quad (12)$$

where the subscript ϕ denotes the parameters of the neural network constituting the encoder. This study proposes utilizing the output from the VAE encoder $q_{\phi}(\cdot)$. The variable \mathbf{z} represents the latent variable, the output from the encoder in the VAE. The output of the encoder corresponding to the observed feature sample,

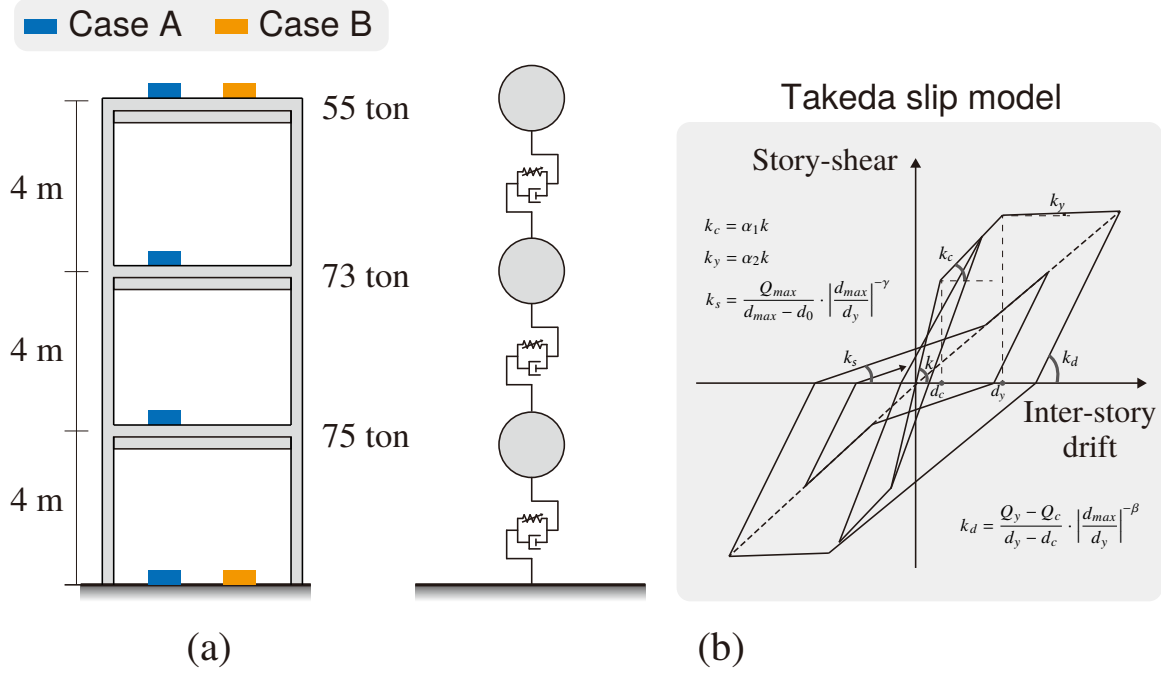


Fig. 1. Three-degree-of-freedom system with the restoring force characteristics of the Takeda-slip model

is articulated as $q_\phi(z|\mathbf{X}_{\text{obs}})$. The latent variable z of the VAE follows a low-dimensional, independent normal distribution, thereby simplifying the integration of Eq. (12). The analytical calculation of Eq. (12) is shown in Appendix Appendix B.

The evaluation of likelihood using the proposed method represents a different interpretation of probability than the distance-based approach. Though the distance-based method quantifies statistical probability based on observations, it is particularly suitable for updating model parameters related to linear responses, provided there is sufficient data. Conversely, the proposed approach introduces a subjective probability obtained from the dataset as prior information. This characteristic makes it effective for updating beliefs with limited observations and is applicable for parameters related to the nonlinear responses of nonlinear models. Hence, both methodologies, each with its unique probability implications, are applicable to diverse situations in model updating, thereby addressing different challenges and objectives.

3. Quantification of Epistemic Uncertainty of MDOF Model Using Observation Variability

In this section, the model updating problem for the multi-degree-of-freedom (MDOF) model is examined to demonstrate the ability of the proposed approach in terms of quantifying the uncertainty resulting from the number of observation points.

3.1. Analysis Model and Input Ground Motion

The validation cases adopted in the numerical experiments in this section and a schematic of the analytical model used are shown in Fig. 1. As shown in Fig. 1(a), a three-story reinforced concrete (RC) structure is considered, and the validation divides into two cases: Case A, where observations are conducted at each floor in addition to the input, and Case B, where observations are made solely at the top floor in addition

Table 1. Assumed model parameters of a MDOF model

k_1 (kN/mm)	k_2 (kN/mm)	k_3 (kN/mm)	d_c (cm)	d_y (cm)	α_1	α_2	β	γ
140	110	60	0.8	4	0.1	0.02	0.4	0.5

to the input. As shown in Fig. 1(b), a three degree of freedom model, which includes the restoring force characteristics of the modified Takeda-slip model (Edo and Takeda, 1977), was created to represent the target structure.

The modified Takeda-slip model provides a comprehensive description of stiffness degradation (also known as slip) in the small drift region caused by the weakening of the column-beam joint anchorage performance. The model is developed based on the Takeda Model (Takeda et al., 1970), which explains the relationship between the displacement and restoring force of reinforced concrete structures. The model parameters are seven and include initial stiffness k , crack displacement d_c , yield displacement d_y , ratio of post-crack stiffness to initial stiffness α_1 , ratio of post-yield stiffness to initial stiffness α_2 , an index to determine the stiffness degradation rate under unloading β , and an index to define the slip behavior γ . The initial stiffness was assumed to vary between stories, whereas to reduce the number of unknown parameters, the other six parameters were assumed to be identical across all the stories. The number of parameters to be updated is nine ($n = 9$). TABLE 1 presents the configuration of the assumed model parameters. The values of k_1 , k_2 , and k_3 in the table correspond with the initial stiffness of the first, second, and third story, respectively. Additionally, cracking and yielding were assumed for occur at 1/500 and 1/100 of the inter-story drift angle, respectively. Commonly used values are assigned to the other model parameters.

The damping constant was set to 4% for the first mode, and was assumed to be proportional to the instantaneous value of the stiffness. Although it is possible to assume the damping constant as one of the unknown model parameters, this study assumes that it is known. The restoring force characteristics affect more on the response at large amplitudes than the damping constant. When implementing the proposed method in actual structures, it is assumed that the damping constants are previously identified using observed data during minor earthquakes through system identification (Verhaegen and Dewilde, 1992).

In this study, a posterior distribution specific to the input ground motion is obtained by using a single observation. The mainshock motion of the 2016 Kumamoto earthquake in Japan, observed at the KMMH16 station of KiK-net (National Research Institute for Earth Science and Disaster Resilience (2019)) in the E-W (East-West) direction with a sampling frequency of 100Hz, is employed as the input ground motion. The duration of the motion is 100 s. The acceleration time history of ground motion utilized, as shown in Fig. 2, records a peak acceleration of 922 gal, thereby meeting the appropriate conditions as an input ground motion of nonlinear response analysis.

The seismic wave was upsampled to a frequency of 1000 Hz. The upsampled wave was then used in the response analysis, thereby resulting in the response wave of each floor. Further, the response waves were downsampled to 100 Hz. To introduce observational noise into the analysis, noise after a normal distribution with a mean of 0 and a standard deviation of 0.1 gal was added to the input wave and to the response wave of each floor. Assuming that these noise-added waves were the ones observed, we proceeded to update the model parameters utilizing the proposed method.

3.2. Dataset and Learning of VAE

The dataset used for training the VAE was created by generating uniform random numbers of the model parameters within the range shown in TABLE 2. In this study, initial stiffness is set to a wide range that encompasses the true value. For application to an actual structure, a design value or a value obtained through

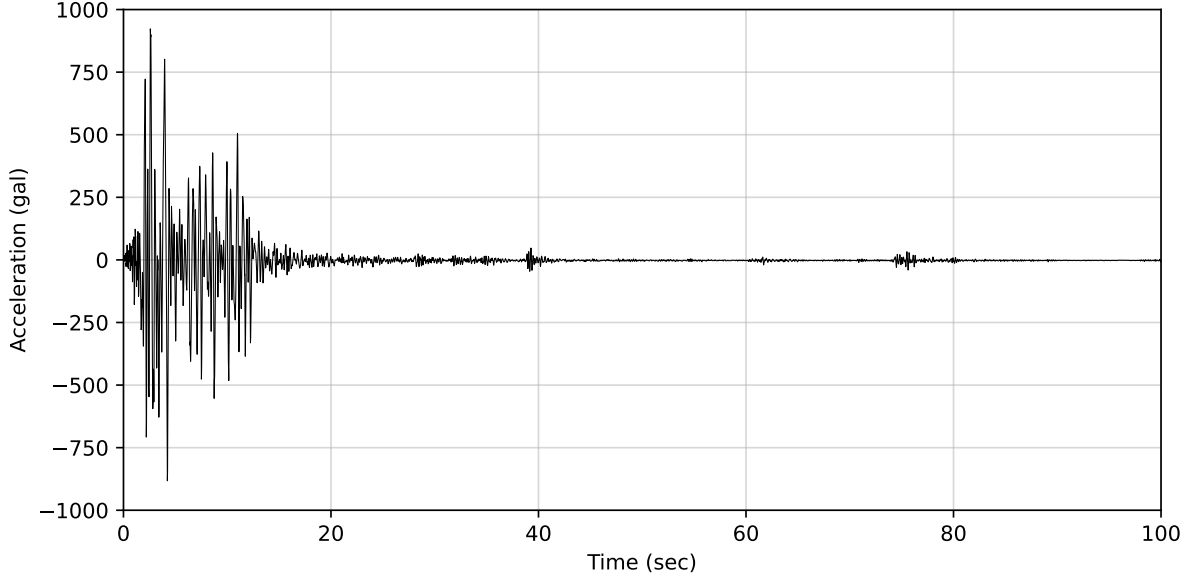


Fig. 2. Waveform of the 2016 Kumamoto Earthquake, observed by the KiK-net strong-motion seismograph network (observation point: KMMH16, direction: E-W)

Table 2. Ranges of model parameters for the MDOF model used in generating the training dataset

	k_1 (kN/mm)	k_2 (kN/mm)	k_3 (kN/mm)	d_c (cm)	d_y (cm)	α_1	α_2	β	γ
upper bound	200	160	120	2	8	0.25	0.05	1	1
lower bound	100	60	20	0.25	2	0.05	0	0	0

system identification (Oku, 2000) would be used in place of the true value. As presented in TABLE 2, the cracking point (first degrading point) is reached within a range of inter-story drift angles of approximately 1/1600 to 1/200, while the yielding point is reached within a range of inter-story drift angles of 1/200 to 1/500. Further, the degrading ratio and slip index were set within a range that includes commonly used values. We set the upper and lower bounds of the model parameters in the same range for both Cases A and B, to discuss how the number of observation points affects the shape of the posterior distribution.

The absolute acceleration of the response obtained from the response analysis was used to determine the frequency response function for the input acceleration, while the real and imaginary parts in the range of 0.1 to 5.24 Hz (512 points) were used as training data. 100,000 data were generated as the training dataset. Here the dataset is formed as a tensor with dimensions (100000, 6, 1, 512), wherein the numbers in the parentheses represent the number of data, the number of channels (corresponding with the real and imaginary parts of frequency response function at each floor), width, and length (corresponding with the frequency point of the frequency response function). In this format, the output size m can be computed as 3072, which is the product of the number of channels, width, and length ($6 \times 1 \times 512$).

The architecture of the VAE network used for model updating is shown in Fig. 3. The VAE comprises an encoder that transforms data \mathbf{X} into a latent variable z , and a decoder that transforms the latent variable z back into data $\hat{\mathbf{X}}$. The encoder has a structure that reduces the dimension of the input through a residual block (He et al., 2016) comprises Convolutional Neural Network (CNN) layers and Fully Connected (FC) layers, while taking the frequency response function as input. The decoder has a symmetrical structure to

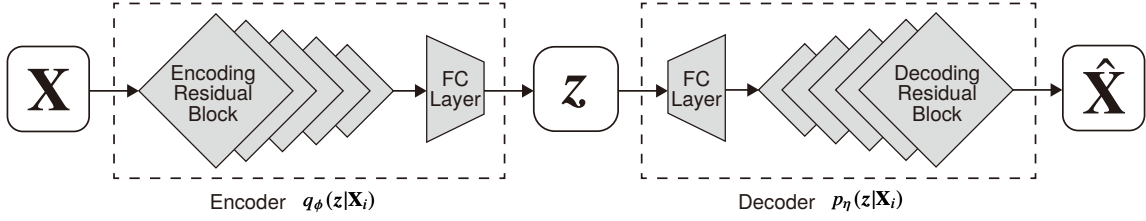


Fig. 3. Architecture of the Variational Auto-encoder (VAE) network for Model updating

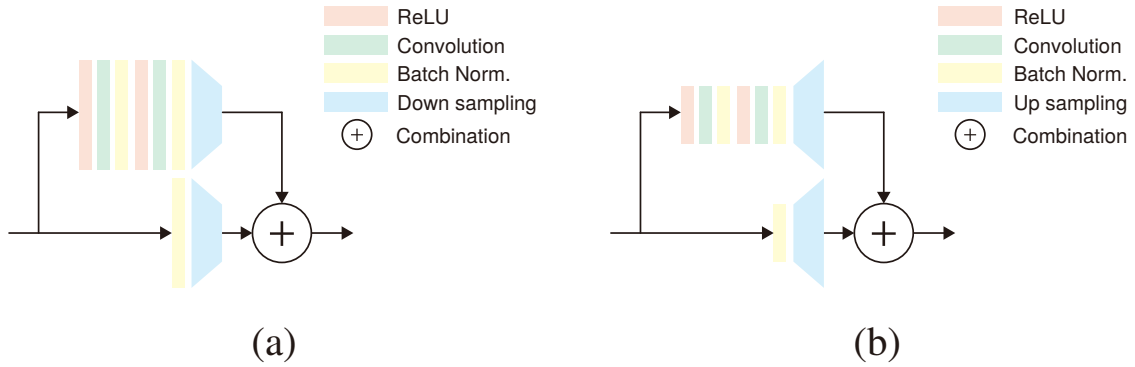


Fig. 4. Residual blocks in the VAE: (a) encoding block, (b) decoding block

the encoder, thereby extending the input dimension of a residual block and FC layers, and using the latent variable as input. The residual blocks for the encoder and decoder are shown in Fig. 4. The encoding residual blocks shown in (a) expand the number of channels while downsampling to reduce the data length. Conversely, the decoding residual blocks shown in (b) reduce the number of channels and increase the length of the data by upsampling. In this study, we set the number of dimensions of the latent variable z to 10, which is slightly more than the nine model parameters. This decision was made based on our assumption that the degree of freedom of the variability of data is at most equivalent to the number of parameters.

The VAE was trained to minimize the loss function (Eq. (A.3) of Appendix Appendix A) using the Adam optimiser (Kingma and Ba, 2015) with a learning rate of 0.0001. We set the batch size to 64 to account for memory capacity, and stopped training after 1,000 epochs while confirming the decrease in the VAE loss function to ensure effective learning.

3.3. Result of Model Updating

The sampling of the model parameters based on the posterior distribution is performed using the Replica Exchange Monte Carlo method (Swendsen and Wang, 1986; Hukushima and Nemoto, 1996), wherein a sample of each replica is generated based on the Metropolis-Hasting method (Metropolis et al., 1953; Hastings, 1970). We set the likelihood function for each replica as follows:

$${}_i\mathcal{LH}({}_i\boldsymbol{\vartheta}) := \{p(\mathbf{X}_{\text{obs}}|{}_i\boldsymbol{\vartheta})\}^{T_i} \quad (13)$$

where ${}_i\boldsymbol{\vartheta}$ is a model parameter vector sample of the i -th replica and T_i is the temperature parameter that determines the form of the likelihood function for the i -th replica. In this study, we established eight replicas

with T_i values of 1, 2, 4, 8, 16, 32, 64, and 128. The exchange of samples between the i -th replica and the j -th replica occurs with the probability $p_e(i, j)$, expressed as:

$$p_e(i, j) := \frac{{}_i\mathcal{LH}(j, \boldsymbol{\theta}) {}_j\mathcal{LH}(i, \boldsymbol{\theta})}{{}_i\mathcal{LH}(i, \boldsymbol{\theta}) {}_j\mathcal{LH}(j, \boldsymbol{\theta})} \quad (14)$$

The exchange according to the acceptance criteria was repeated 1,000 times for every 100 samples to obtain a total of 100,000 samples. The initial sample for each replica was generated so that the corresponding sample in the space of latent variable is close to that of observation. Setting the initial value in this way makes convergence faster and allows the burn-in period to be set short. To verify the validity of the likelihood evaluation using the proposed method, the prior distribution was set as a non-informative distribution.

The first 10,000 samples were considered as burn-in and hence were removed. The samples were further thinned by retaining every 30th sample from the remaining samples, thereby resulting in a total of 3,000 samples. The shape of the posterior distribution, obtained by 1-dimensional Gaussian kernel density estimation, was determined using the 3,000 retained samples as shown in Fig. 5.

In both validation cases, distributions that include the true values were successfully obtained for the posterior distributions of the nine model parameters. Narrow and sharp distributions were obtained for the initial stiffness, which are related to linear response and have a dominant impact on the response. However, parameters influencing only on the nonlinear response, such as stiffness reduction rates or slip index, had posterior distributions with a wider shape. In Case B, where there are less number of observations available, the distribution peaks were slightly shifted away from the true value than those of Case A, where there are more observations available. In Case B, where the number of observations is smaller (uncertainty is larger), the breadths of the posterior distribution of most parameters were wider, and the peaks were lower than those of Case A. These results suggest that the proposed method not only facilitates the high-accuracy updating of multiple parameters related to complex nonlinear responses but also quantitatively reflects uncertainty due to the lack of information originating from the number of observations.

4. Quantification of uncertainty due to lack of information on nonlinear response

The relationship between the degree of nonlinearity of the response and breadths of the posterior distribution of the model parameters is explored using our proposed method. When severity of input ground motion decreases, information about the nonlinear response decrease from the observed records. For demonstration purposes, we utilize a single-degree-of-freedom shear spring model, as illustrated in Fig. 6. It is characterized by its bilinear restoring force and a relatively small number of parameters, thereby serving as an ideal example for validating our approach.

4.1. Target Analysis Model and Input Ground Motion

The model parameters comprise the natural frequency, which indicates the initial stiffness, the yield displacement, which indicates the displacement at the yield point, and the degrading ratio, which represents the post-yield stiffness relative to the initial stiffness ($n = 3$). These three parameters establish the bilinear restoring force characteristics. Here, the damping constant is assumed to be known, as in the previous example. The model parameters for the validation model group utilized in the numerical experiment are presented in TABLE 3. The group of validation models, comprising 45 models with an identical natural frequency of 2Hz, parameterizes nine yield displacement ratios and five degrading ratios. The yield displacement ratio, expressed as a ratio to the maximum displacement obtained through linear response analysis, was used to measure the yield displacement. The response analyses were conducted by employing

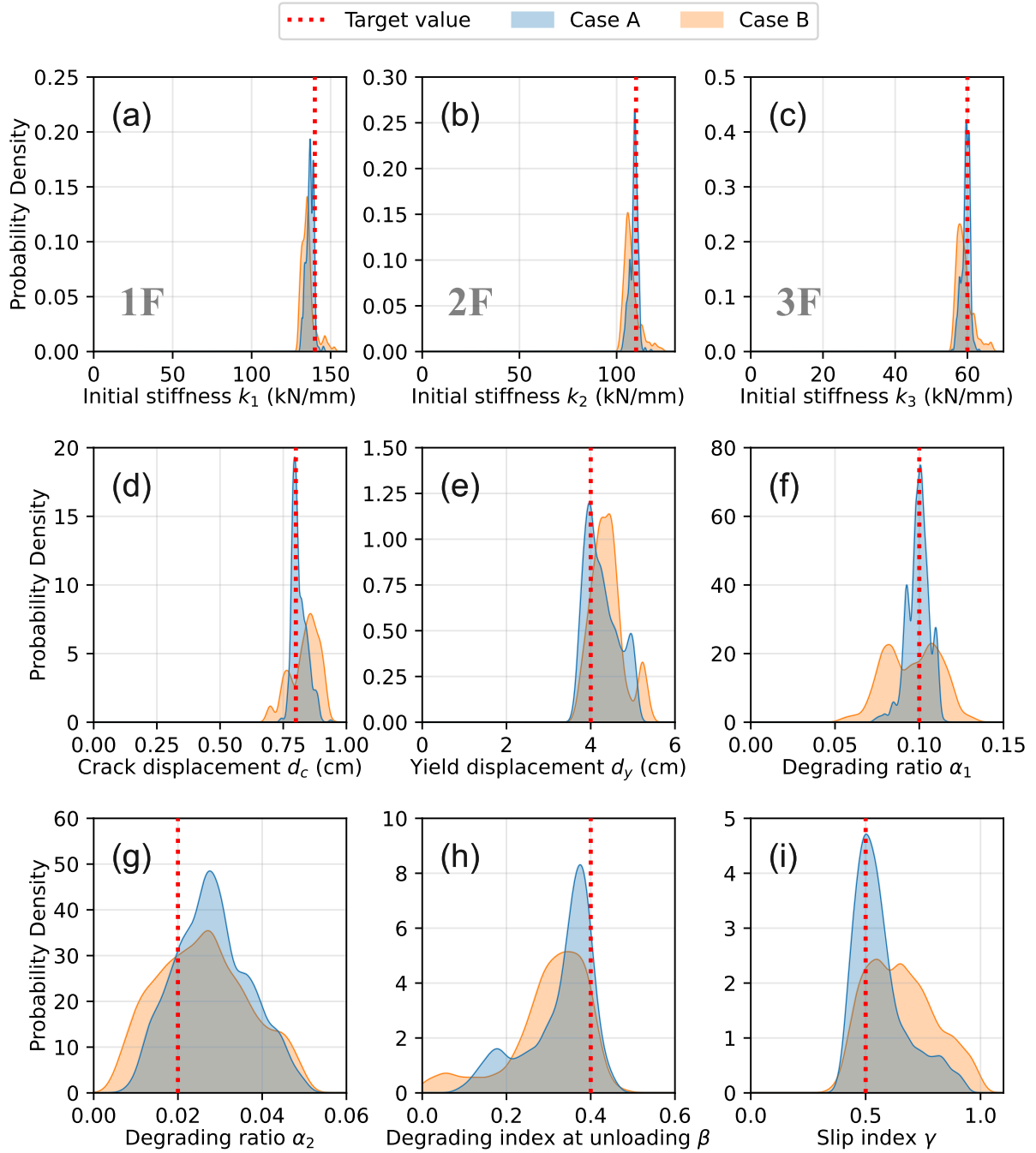


Fig. 5. Comparison of posterior distributions for model parameters in Cases A and B

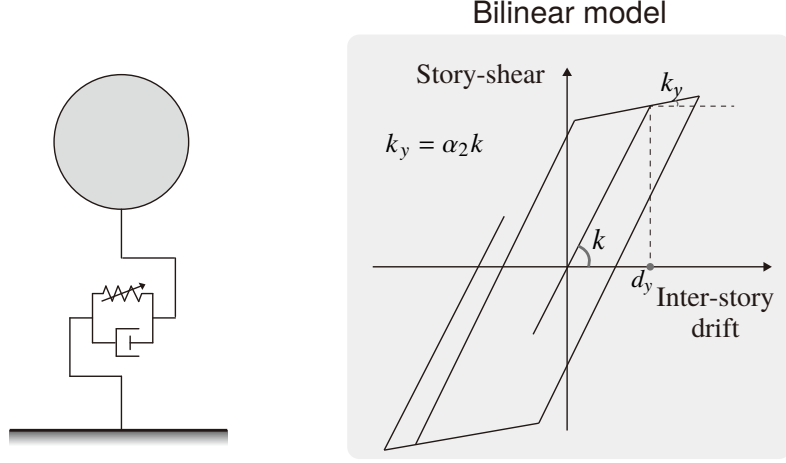


Fig. 6. Single-degree-of-freedom system with the restoring force characteristics of bilinear model

Table 3. Assumed model parameters of validation models

Natural frequency (Hz)	Yield displacement ratio	Degrading ratio
2	0.5, 0.55, 0.6, 0.65, 0.7, 0.75, 0.8, 0.85, 0.9	0.001, 0.1, 0.2, 0.3, 0.4

the identical input ground motion as in the previous example (see Fig. 2), to acquire the waveform of response acceleration. The damping constant was set to 5%, and the sampling period was upsampled to an interval of 0.001s. The acceleration waveform obtained was presumed to have been observed incorporating observation noise (identical to previous example), and the model parameters were updated using the proposed method.

4.2. Dataset and Learning of VAE

The training dataset for the VAE was created using numerous response analysis models to obtain frequency response functions. To construct these response analysis models, we generated uniform random numbers of the model parameters within the ranges, as presented in TABLE 4. By configuring TABLE 4, half of the dataset comprises data that exhibits nonlinearity. The response analyses were conducted using the same input ground motion that was used for the target models. The damping constant is assumed to be known, following the same approach as in the previous example. The frequency response function was obtained relative to the input acceleration using the absolute acceleration of the response obtained from the response analysis. The real and imaginary components of the 512 dimensions within the frequency range of 0.1 to 5.22 Hz in the frequency response function were allocated to the corresponding channels in the training dataset. A total of 100,000 frequency response functions were generated for the training dataset. The dataset is formed as a tensor with dimensions (100000, 2, 1, 512), where the numbers in the parentheses represent the number of data, number of channels, width, and length. Using this format, the output size m can be computed as 1024, which is the product of the number of channels, width, and length ($2 \times 1 \times 512$).

In this study, the employed VAE uses the same configuration as described in the previous example,

Table 4. Ranges of model parameters for the SDOF model used in generating the training dataset

model parameter	Natural frequency (Hz)	Yield displacement ratio	Degrading ratio
upper bound	5	1.8	0.5
lower bound	0.5	0.2	0

including maintaining a latent variable dimension of 10, as illustrated in Fig. 3. Based on the aforementioned procedures outlined, the training of the VAE was conducted using the Adam optimizer with a learning rate of 0.0001. Due to memory capacity considerations, we set a batch size of 64. The decision to train for 1000 epochs was based on monitoring the decrease in the loss function of VAE, which is further detailed in Appendix Appendix A.

4.3. Result of Model Updating

Consistent with the methodology outlined in the previous example, the MCMC simulation in this chapter was conducted using the observed waveforms from the 45 validation models. The conditions of the MCMC simulation, including the selection of starting samples and the number of sampling iterations, were identical to those previously described. Samples were obtained based on the posterior distribution, thereby maintaining a similar procedural fidelity as established in the aforementioned section. Although visualising the posterior distributions of all 45 models is omitted for space reasons, the relatively simple model parameter updating problem facilitated very accurate estimations.

For this validation, our main objective is to examine the trends in uncertainty evaluation, particularly those attributed to limited information, without focusing on assessing the estimation accuracy. The breadth of the posterior distribution is determined as the sample standard deviation by Eq. (15) and displayed against the yield displacement ratio, as shown in Fig.7.

$$\sigma_i = \sqrt{\frac{1}{n_s} \sum_{j=1}^{n_s} \left({}_1\vartheta_i^{(j)} - {}_1\bar{\vartheta}_i \right)^2} \quad (15)$$

Here, the number of MCMC adopted samples is denoted as n_s , whereas ${}_1\vartheta_i^{(j)}$ represents the i -th model parameter of the j -th sample of the 1st replica. Additionally, ${}_1\bar{\vartheta}_i$ represents the mean of the series ${}_1\vartheta_i^{(j)}$, as expressed as follows:

$${}_1\bar{\vartheta}_i = \frac{1}{n_s} \sum_{j=1}^{n_s} {}_1\vartheta_i^{(j)} \quad (16)$$

The values on the horizontal axis of Fig. 7 correspond with the target values of the yield displacement ratio, and the colours of the graph correspond with the target values of the degrading ratio α . An increase in the prescribed values of the yield displacement ratio and degrading ratio results in a decrease in nonlinearity of response. This could be perceived as an increase in uncertainty due to insufficient data on the nonlinear response. The natural frequency, which draws information from the complete time domain of the response data, is indicative of a consistently negligible breadth of the posterior distribution throughout the range. Conversely, the yield displacement ratio and degrading ratio, which obtain information from the nonlinear response, exhibited a tendency for the breadth of the posterior distribution to increase as the target values of the yield displacement ratio and degrading ratio increased. These findings show that the proposed technique accounts for the uncertainty arising from insufficient information on the nonlinear response and adjusts the breadth of the posterior distribution accordingly.

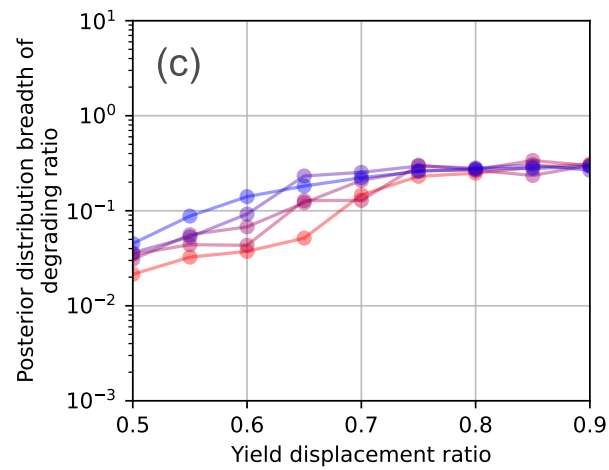
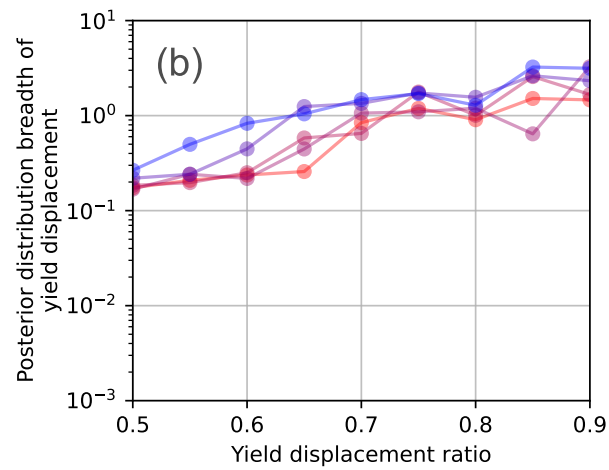
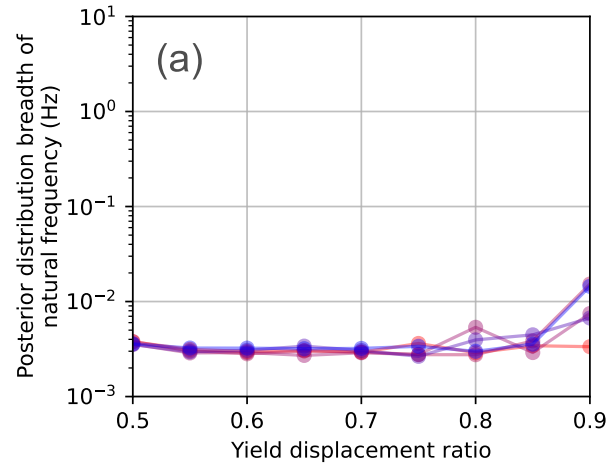
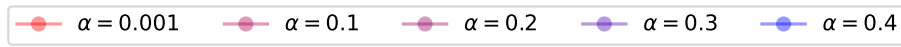


Fig. 7. Variation of posterior distribution breadth for validation models

5. Conclusion

This study proposed a novel Bayesian technique for updating the parameters of a nonlinear response analysis model. This technique considers the lack of information due to limited number of observations by employing a variational auto-encoder. We conducted numerical experiments to investigate the shape of the posterior distribution of model parameters, thereby validating the proposed methodology. The numerical experiments were conducted using a multi-degree-of-freedom system with a modified Takeda-slip hysteresis characteristics model, which exhibits relatively complex hysteresis features. It was confirmed that the proposed approach successfully attained posterior distributions close to the target values. The shape of the posterior distribution depends on the density of observations. The numerical experiments conducted using a single-degree-of-freedom system with a bilinear hysteresis model, which exhibits relatively simple hysteresis features. The shape of the posterior distribution also depends on the degree of nonlinearity in observed records. These results show that the proposed method can evaluate likelihood effectively, hereby considering uncertainty due to limited information. This study introduced a rigorous procedure for calculating likelihood, employing MCMC with response analysis, which requires relatively large computational resources. Developing a methodology to reduce such computational resources will be the focus of future research.

6. Data Availability Statement

All data, models, or code that support the findings of this study are available from the corresponding author upon reasonable request.

Appendix A. Overview of Variational Auto-encoder

The proposed method utilizes variational auto-encoders (VAEs) (Kingma and Welling, 2014). These are generative models that aim to replicate the distribution of a training dataset from a latent variable. An architecture of a VAE, as illustrated in Fig. A.8, comprises two main components: an encoder and a decoder. The encoder, a neural network, transforms the input data \mathbf{X} into a latent variable \mathbf{z} . The decoder, another neural network, uses this latent variable to reconstruct data $\hat{\mathbf{X}}$ that reconstruct the original input in dimensions.

Although VAEs are similar to conventional autoencoders (Hinton and Salakhutdinov, 2006), VAEs treat the outputs of the encoder and decoder as random variables individually. This is achieved by what is known as the reparameterization trick. In this approach, the standard deviation of output from the encoder σ is multiplied with a random number ϵ , drawn from the multi-variate standard normal distribution. Later, the mean μ is added to generate the random vector \mathbf{z} . The reparameterization trick enables the backpropagation of gradients through random nodes, thereby facilitating the training of the neural network.

The decoder in a VAE aims to optimize the likelihood $p_\eta(\mathbf{X})$ reproducing the input data \mathbf{X} . Due to the intractability of $p_\eta(\mathbf{X}|\mathbf{z})$, the output of the encoder $q_\phi(\mathbf{z}|\mathbf{X})$, which approximates the likelihood of \mathbf{z} for a given \mathbf{X} , is utilized instead. Here, ϕ and η represent the parameters of the encoder and decoder neural networks, respectively.

For each training instance \mathbf{X}_i , the output of the decoder $p_\eta(\mathbf{X}_i)$ is independent of \mathbf{z} and follows the distribution $q_\phi(\mathbf{z}|\mathbf{X}_i)$. This relationship is expressed in Eq. (A.1):

$$\log p_\eta(\mathbf{X}_i) = \mathcal{L}(\eta, \phi, \mathbf{X}_i) + D_{KL}(q_\phi(\mathbf{z}|\mathbf{X}_i) || p_\eta(\mathbf{z}|\mathbf{X}_i)) \geq \mathcal{L}(\eta, \phi, \mathbf{X}_i) \quad (\text{A.1})$$

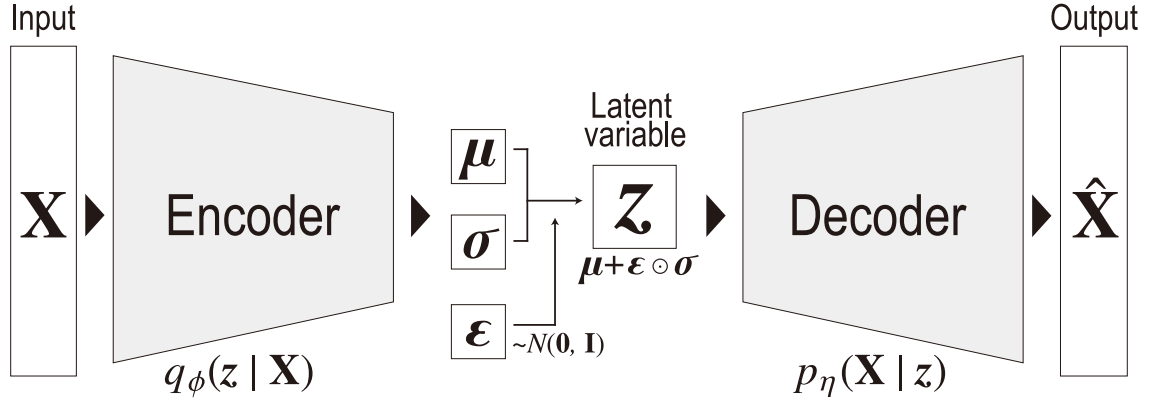


Fig. A.8. VAE architecture

where D_{KL} denotes the Kullback-Leibler divergence. In the context of VAEs, an error function is defined as expressed in Eq. (A.2). The neural network parameters ϕ and η are fine-tuned to minimize this error function.

$$-\mathcal{L}(\eta, \phi, \mathbf{X}_i) = -\mathbb{E}_{q_\phi(\mathbf{z}|\mathbf{X}_i)} [\log p_\eta(\mathbf{X}_i|\mathbf{z})] + D_{KL}(q_\phi(\mathbf{z}|\mathbf{X}_i) || p_\eta(\mathbf{z})) \quad (\text{A.2})$$

In this equation, $\mathbb{E}_{q_\phi(\mathbf{z}|\mathbf{X}_i)} [\cdot]$ represents the expected value operation for the variable \mathbf{z} .

The first term on the right-hand side of Eq. (A.2) represents the reconstruction error, with the aim to align the output of the decoder with the input data \mathbf{X}_i . This alignment is approximated using the Monte Carlo method, wherein the random number $z_{i,l}$ drawn from $q_\phi(\mathbf{z}|\mathbf{X}_i)$ is employed, as follows :

$$-\mathbb{E}_{q_\phi(\mathbf{z}|\mathbf{X}_i)} [\log p_\eta(\mathbf{X}_i|\mathbf{z})] \approx -\frac{1}{L} \sum_{z_{i,l}} \log p_\eta(\mathbf{X}_i|z_{i,l}) \quad (\text{A.3})$$

where, L represents the number of samples used in the Monte Carlo estimation. In mini-batch learning, wherein training data is segmented into smaller batches for processing, it's normal to set $L = 1$ when the batch size (indicating the data count in each batch) is adequately large (as suggested in the original paper, it is 100). To compute $\log p_\eta(\mathbf{X}_i|z_{i,l})$, one must define a loss function for the output data of the decoder. Cross-entropy loss is used for discrete datasets, whereas mean square error is preferred for continuous data. In this study, we employ the mean square error due to the nature of our continuous data.

The second term in Eq. (A.2) acts as a regularization factor, thereby ensuring the output of the encoder $q_\phi(\mathbf{z}|\mathbf{X}_i)$ closely approximates $p_\eta(\mathbf{z})$, modeled as a standard normal distribution. By training the encoder to transform the input data \mathbf{X} into independent standard normal variable \mathbf{z} in a nonlinear manner, the likelihood evaluation method is established. It is important to note that this assumption does not rely on previously observed data or model parameter distributions but rather defines the learning process of VAEs.

Appendix B. Analytical Method for Likelihood Computation

In this appendix, we detail the analytical method for computing likelihoods. As the latent variable \mathbf{z} is trained to conform to a multi-dimensional standard normal distribution, we decompose and integrate each

dimension as delineated below:

$$\int_{\mathbf{Z}} \frac{q_{\phi}(\mathbf{z}|\mathbf{X}_{\text{obs}}) q_{\phi}(\mathbf{z}|\mathbf{X}_{\text{sim}})}{q_{\phi}(\mathbf{z})} d\mathbf{z} = \prod_{i=1}^{zdim} \int_{-\infty}^{\infty} \frac{q_{\phi}(z_i|\mathbf{X}_{\text{obs}}) q_{\phi}(z_i|\mathbf{X}_{\text{sim}})}{q_{\phi}(z_i)} dz_i \quad (\text{B.1})$$

The integration over each dimension of the latent variable is further examined, as expressed in Eq. (B.2):

$$\int_{-\infty}^{\infty} \frac{q_{\phi}(z_i|\mathbf{X}_{\text{obs}}) q_{\phi}(z_i|\mathbf{X}_{\text{sim}})}{q_{\phi}(z_i)} dz_i =: L_{z_i} \quad (\text{B.2})$$

where $q_{\phi}(z_i | \mathbf{X}_{\text{obs}})$ and $q_{\phi}(z_i | \mathbf{X}_{\text{sim}})$ represent encoder outputs and are thereby modeled as normal distributions via the reparameterization trick. The term $q_{\phi}(z_i)$ approximates a normal distribution due to the regularization error component. Assuming $z_i|\mathbf{X}_{\text{obs}} \sim N(\mu_1, \sigma_1)$, $z_i|\mathbf{X}_{\text{sim}} \sim N(\mu_2, \sigma_2)$, $z_i \sim N(\mu_3, \sigma_3)$, the term L_{z_i} can be expressed as:

$$L_{z_i} = \sqrt{\frac{3\sigma_i^2}{2\pi_1\sigma_i^2\sigma_i^2}} \int_{-\infty}^{\infty} e^{-\frac{(z_i-\mu_1)^2}{2\sigma_1^2} - \frac{(z_i-\mu_2)^2}{2\sigma_2^2} + \frac{(z_i-\mu_3)^2}{2\sigma_3^2}} dz_i \quad (\text{B.3})$$

As expressed in Eq. (B.3), the exponential portion becomes a quadratic polynomial, further simplifying the expression as in Eq. (B.4).

$$L_{z_i} = d_i \int_{-\infty}^{\infty} e^{-(a_i z_i^2 + b_i z_i + c_i)} dz_i \quad (\text{B.4})$$

Regarding the coefficients, we have $a_i = \frac{1}{2\sigma_1^2} + \frac{1}{2\sigma_2^2} - \frac{1}{2\sigma_3^2}$, $b_i = -\frac{\mu_1}{\sigma_1^2} - \frac{\mu_2}{\sigma_2^2} + \frac{\mu_3}{\sigma_3^2}$, $c_i = \frac{\mu_1^2}{2\sigma_1^2} + \frac{\mu_2^2}{2\sigma_2^2} - \frac{\mu_3^2}{2\sigma_3^2}$, $d_i = \sqrt{\frac{3\sigma_i^2}{2\pi_1\sigma_i^2\sigma_i^2}}$. As $\sigma_1, \sigma_2 \ll \sigma_3$, it follows that $a_i > 0$.

The equation transforms as follows:

$$L_{z_i} = d_i e^{\frac{b_i^2 - 4a_i c_i}{4a_i}} \sqrt{\frac{\pi}{a_i}} \int_{-\infty}^{\infty} \sqrt{\frac{a_i}{\pi}} e^{-a_i \left(z_i + \frac{b_i}{2a_i}\right)^2} dz_i \quad (\text{B.5})$$

The integrand within the integral represents a normal distribution with mean $-\frac{b_i}{2a_i}$ and standard deviation $\sqrt{\frac{1}{2a_i}}$, culminating in the result as in Eq. (B.6).

$$L_{z_i} = d_i e^{\frac{b_i^2 - 4a_i c_i}{4a_i}} \sqrt{\frac{\pi}{a_i}} \quad (\text{B.6})$$

The process, as summarized in Eq. (B.7), involves breaking down the complex integrals into more manageable expressions for each dimension of \mathbf{z} .

$$\int_{\mathbf{Z}} \frac{q_{\phi}(\mathbf{z}|\mathbf{X}_{\text{obs}}) q_{\phi}(\mathbf{z}|\mathbf{X}_{\text{sim}})}{q_{\phi}(\mathbf{z})} d\mathbf{z} = \prod_{i=1}^{zdim} d_i e^{\frac{b_i^2 - 4a_i c_i}{4a_i}} \sqrt{\frac{\pi}{a_i}} \quad (\text{B.7})$$

References

Beck, J.L., Katafygiotis, L.S., 1998. Updating models and their uncertainties. i: Bayesian statistical framework. *Journal of Engineering Mechanics* 124, 455–461. doi:10.1061/(ASCE)0733-9399(1998)124:4(455).

- Bhattacharyya, A., 1946. On a measure of divergence between two multinomial populations. *Indian Statistical Institute* 157, 869. doi:<https://doi.org/10.1038/157869b0>.
- Bi, S., Broggi, M., Beer, M., 2019. The role of the bhattacharyya distance in stochastic model updating. *Mechanical Systems and Signal Processing* 117, 437–452. doi:<https://doi.org/10.1016/j.ymssp.2018.08.017>.
- Bi, S., Prabhu, S., Cogan, S., Atamturktur, S., 2017. Uncertainty quantification metrics with varying statistical information in model calibration and validation. *AIAA Journal* 55, 3570–3583. doi:10.2514/1.J055733.
- Collins, J.D., Hart, G.C., Hasselman, T.K., Kennedy, B., 1974. Statistical identification of structures. *AIAA Journal* 12, 185–190. URL: <https://doi.org/10.2514/3.49190>, doi:10.2514/3.49190.
- Edo, H., Takeda, T., 1977. Elastoplastic seismic response frame analysis of reinforced concrete structures: Structural systems (in Japanese). *Summaries of Technical Papers of Annual Meeting* 52, 1877–1878. URL: <https://cir.nii.ac.jp/crid/1573950401726246912>. original article in Japanese.
- Goldstein, M., 2006. Subjective Bayesian Analysis: Principles and Practice. *Bayesian Analysis* 1, 403 – 420. URL: <https://doi.org/10.1214/06-BA116>, doi:10.1214/06-BA116.
- Hastings, W.K., 1970. Monte carlo sampling methods using markov chains and their applications. *Biometrika* 57, 97–109. URL: <http://www.jstor.org/stable/2334940>.
- He, K., Zhang, X., Ren, S., Sun, J., 2016. Deep residual learning for image recognition, in: 2016 IEEE Conference on Computer Vision and Pattern Recognition (CVPR), pp. 770–778. doi:10.1109/CVPR.2016.90.
- Hinton, G.E., Salakhutdinov, R.R., 2006. Reducing the dimensionality of data with neural networks. *science* 313, 504–507. doi:10.1126/science.1127647.
- Hinze, M., Schmidt, A., Leine, R., 2020. The direct method of lyapunov for nonlinear dynamical systems with fractional damping. *Nonlinear Dynamics* 102, 1–21. doi:10.1007/s11071-020-05962-3.
- Hukushima, K., Nemoto, K., 1996. Exchange monte carlo method and application to spin glass simulations. *Journal of the Physical Society of Japan* 65, 1604–1608. URL: <https://doi.org/10.1143/JPSJ.65.1604>, doi:10.1143/JPSJ.65.1604.
- Imregun, M., Visser, W.J., Ewins, D., 1995. Finite element model updating using frequency response function data: I. theory and initial investigation. *Mechanical Systems and Signal Processing* 9, 187–202. URL: <https://www.sciencedirect.com/science/article/pii/S0888327085700155>, doi:<https://doi.org/10.1006/mssp.1995.0015>.
- Kingma, D.P., Ba, J., 2015. Adam: A method for stochastic optimization, in: Bengio, Y., LeCun, Y. (Eds.), 3rd International Conference on Learning Representations, ICLR 2015, San Diego, CA, USA, May 7-9, 2015, Conference Track Proceedings. URL: <http://arxiv.org/abs/1412.6980>.
- Kingma, D.P., Welling, M., 2014. Auto-encoding variational bayes, in: Bengio, Y., LeCun, Y. (Eds.), 2nd International Conference on Learning Representations, ICLR 2014, Banff, AB, Canada, April 14-16, 2014, Conference Track Proceedings. URL: <http://arxiv.org/abs/1312.6114>.
- Kitahara, M., Bi, S., Broggi, M., Beer, M., 2021. Bayesian model updating in time domain with metamodel-based reliability method. *ASCE-ASME Journal of Risk and Uncertainty in Engineering Systems, Part A: Civil Engineering* 7, 04021030. doi:10.1061/AJRUA6.0001149.
- Kitahara, M., Bi, S., Broggi, M., Beer, M., 2022. Nonparametric bayesian stochastic model updating with hybrid uncertainties. *Mechanical Systems and Signal Processing* 163, 108195. URL: <https://www.sciencedirect.com/science/article/pii/S0888327021005719>, doi:<https://doi.org/10.1016/j.ymssp.2021.108195>.
- Metropolis, N., Rosenbluth, A., Rosenbluth, M., Teller, A., Teller, E., 1953. Equation of state calculations by fast computing machines. *The journal of chemical physics* 21, 1087–1092.
- Mottershead, J.E., Link, M., Friswell, M.I., 2011. The sensitivity method in finite element model updating: A tutorial. *Mechanical Systems and Signal Processing* 25, 2275–2296. URL: <https://www.sciencedirect.com/science/article/pii/S0888327010003316>, doi:<https://doi.org/10.1016/j.ymssp.2010.10.012>.
- National Research Institute for Earth Science and Disaster Resilience (2019), . NIED K-NET, KiK-net. doi:<https://www.doi.org/10.17598/NIED.0004>.
- Oku, H., 2000. Equential subspace state-space system identification and state estimation of unknown multivariable systems. Ph.D. thesis. The University of Tokyo. Tokyo, Japan.
- Saito, T., 2013. Evaluation of seismic response of buildings and probabilistic damage estimation applying bayesian model updating (in Japanese). *Journal of Structural and Construction Engineering (Transactions of AIJ)* 78, 61–70. doi:10.3130/aijs.78.61.
- Saito, T., Beck, J.L., 2010. Bayesian model selection for arx models and its application to structural health monitoring. *Earthquake Engineering & Structural Dynamics* 39, 1737–1759. URL: <https://onlinelibrary.wiley.com/doi/abs/10.1002/eqe.1006>, doi:<https://doi.org/10.1002/eqe.1006>.
- Supple, J.D., Sanayei, M., 2014. Finite element model updating using frequency response functions and numerical sensitivities. *Structural Control and Health Monitoring* 21, 784–802. URL: <https://onlinelibrary.wiley.com/doi/abs/10.1002/stc.1601>, doi:<https://doi.org/10.1002/stc.1601>, arXiv:<https://onlinelibrary.wiley.com/doi/pdf/10.1002/stc.1601>.

- Song, M., Renson, L., Noël, J., Moaveni, B., Kerschen, G., 2018. Bayesian model updating of nonlinear systems using nonlinear normal modes. *Structural Control and Health Monitoring* 25, e2258. URL: <https://onlinelibrary.wiley.com/doi/abs/10.1002/stc.2258>, doi:<https://doi.org/10.1002/stc.2258>.
- Swendsen, R.H., Wang, J., 1986. Replica monte carlo simulation of spin-glasses. *Phys. Rev. Lett.* 57, 2607–2609. doi:10.1103/PhysRevLett.57.2607.
- Takeda, T., Sozen, M., Nielsen, N., 1970. Reinforced concrete response to simulated earthquakes. *Journal of the structural division (ASCE)* 96, 2557–2573.
- Verhaegen, M., Dewilde, P., 1992. Subspace model identification. *International Journal of Control* 56, 1187–1210.
- Volodina, V., Challenor, P., 2021. The importance of uncertainty quantification in model reproducibility. *Philosophical Transactions of the Royal Society A: Mathematical, Physical and Engineering Sciences* 379, 20200071. URL: <https://royalsocietypublishing.org/doi/abs/10.1098/rsta.2020.0071>, doi:10.1098/rsta.2020.0071, arXiv:<https://royalsocietypublishing.org/doi/pdf/10.1098/rsta.2020.0071>.
- Yang, S., Yi, T., Qu, C., Zhang, S., Li, C., 2023. Adaptive sampling-based bayesian model updating for bridges considering substructure approach. *ASCE-ASME Journal of Risk and Uncertainty in Engineering Systems, Part A: Civil Engineering* 9, 04023024. doi:10.1061/AJRUA6.RUENG-1077.